J. Fluid Mech. (2012), *vol.* 704, *pp.* 280–300.
doi:10.1017/jfm.2012.238

Perturbation response and pinch-off of vortex rings and dipoles

Clara O'Farrell[1]† **and John O. Dabiri**[2]

[1] Control and Dynamical Systems, California Institute of Technology, Pasadena, CA 91125, USA

[2] Graduate Aeronautical Laboratories and Bioengineering, California Institute of Technology, Pasadena, CA 91125, USA

(Received 7 November 2011; revised 11 May 2012; accepted 17 May 2012; first published online 29 June 2012)

The nonlinear perturbation response of two families of vortices, the Norbury family of axisymmetric vortex rings and the Pierrehumbert family of two-dimensional vortex pairs, is considered. Members of both families are subjected to prolate shape perturbations similar to those previously introduced to Hill's spherical vortex, and their response is computed using contour dynamics algorithms. The response of the entire Norbury family to this class of perturbations is considered, in order to bridge the gap between past observations of the behaviour of thin-cored members of the family and that of Hill's spherical vortex. The behaviour of the Norbury family is contrasted with the response of the analogous two-dimensional family of Pierrehumbert vortex pairs. It is found that the Norbury family exhibits a change in perturbation response as members of the family with progressively thicker cores are considered. Thin-cored vortices are found to undergo quasi-periodic deformations of the core shape, but detrain no circulation into their wake. In contrast, thicker-cored Norbury vortices are found to detrain excess rotational fluid into a trailing vortex tail. This behaviour is found to be in agreement with previous results for Hill's spherical vortex, as well as with observations of pinch-off of experimentally generated vortex rings at long formation times. In contrast, the detrainment of circulation that is characteristic of pinch-off is not observed for Pierrehumbert vortex pairs of any core size. These observations are in agreement with recent studies that contrast the formation of vortices in two and three dimensions. We hypothesize that transitions in vortex formation, such as those occurring between wake shedding modes and in vortex pinch-off more generally, might be understood and possibly predicted based on the observed perturbation responses of forming vortex rings or dipoles.

Key words: contour dynamics, vortex dynamics, vortex instability

1. Introduction

A variety of biological and engineering flows are characterized by the presence of axisymmetric vortex rings. Most commonly, these vortex rings are observed in starting or pulsed axisymmetric jets, where a fluid column is ejected through a circular nozzle or aperture. As fluid is ejected, boundary layer separation at the aperture leads to roll-up and the formation of a vortex ring. Gharib, Rambod & Shariff (1998) found that vortex rings cannot grow indefinitely, as there is a physical limit to their size.

† Email address for correspondence: ofarrell@cds.caltech.edu

Beyond this limit, the vortex rings reject additional vorticity, which forms a wake of Kelvin–Helmholtz-type vortices that trail behind the ring.

Gharib *et al.* (1998) explained this transition in terms of a variational principle due to Kelvin and Benjamin (Benjamin 1976; Kelvin 1880*b*), which states that a vortex ring is a steady solution to the equations of motion only when it has maximum energy with respect to rearrangements of the vorticity that preserve the same total impulse. Subsequently, several models predicting pinch-off have been proposed, including those of Mohseni & Gharib (1998), Shusser & Gharib (2000), Linden & Turner (2001), Kaplansky & Rudi (2005) and Gao & Yu (2010). In addition, Krueger & Gharib (2003) have demonstrated that the pinch-off process has dynamical significance, as the efficiency of momentum transport in pulsed jets is optimized when the size of the vortex rings generated by the jet is maximized.

Notably, both the argument of Gharib *et al.* (1998) and the aforementioned models make use of a family of vortex rings introduced by Norbury (1973), as a model for axisymmetric vortex rings. The Norbury family consists of steadily translating axisymmetric vortex rings with finite core size, ranging from classical thin-cored vortices to Hill's spherical vortex. In all members of the family, the vorticity density (ω/r, where r is the radial coordinate) is constant inside the core. These vortex rings serve as a low-order model of experimentally generated vortex rings of different core sizes. Despite its simplicity, the Norbury family of vortex rings has been successfully employed as a model for axisymmetric vortex rings at different stages in their development (Gharib *et al.* 1998; Mohseni & Gharib 1998; Shusser & Gharib 2000; Linden & Turner 2001; Kaplansky & Rudi 2005; Gao & Yu 2010).

That Hill's spherical vortex and nearly spherical members of the Norbury family are the solution to a maximization problem on the energy function as outlined by Benjamin (1976) was shown by Wan (1988). Moffatt & Moore (1978) considered the linear stability of Hill's spherical vortex subjected to axisymmetric perturbations, and found that these decay everywhere except in a region near the rear stagnation point, where a tail of growing length develops. Building on this analysis, Pozrikidis (1986) studied the nonlinear instability of Hill's spherical vortex to axisymmetric shape perturbations of finite size. When subjected to an axisymmetric prolate perturbation, Pozrikidis (1986) found that Hill's vortex returned to a smaller spherical vortex by detraining rotational fluid into a tail. Gharib *et al.* (1998) noted that this circulation shedding is analogous to pinch-off. In contrast, Ye & Chu (1995) investigated the response of a member of the Norbury family of moderate core thickness to similar shape perturbations, and found no evidence of tail shedding. However, the nonlinear response of the remainder of the Norbury family to prolate shape perturbations is unknown, and the transition from the observations of Ye & Chu (1995) to those of Pozrikidis (1986) has not been previously characterized.

In two-dimensional flows, a coherent structure similar to the axisymmetric vortex ring is often observed: the symmetric vortex dipole. Dipolar vortices have been observed experimentally in flows in which three-dimensional motions have been suppressed by stratification (van Heijst & Flór 1989), by utilizing a thin soap film (Couder & Basdevant 1986; Afanasyev 2006), by rotation of the ambient fluid (Velasco Fuentes & van Heijst 1994; Trieling *et al.* 2010), or by the imposition of a magnetic field on a layer of mercury (Nguyen Duc & Sommeria 1998). In these experiments and in computational studies (van Geffen & van Heijst 1998; Duran-Matute *et al.* 2010; Pedrizzetti 2010), thick-cored, nearly symmetry-axis-touching dipoles were often observed, leading to speculation that the physical constraint on vortex growth identified by Gharib *et al.* (1998) for axisymmetric vortex rings does not extend to two-dimensional vortex pairs. Nitsche (2001) also found a difference in the

behaviour of axisymmetric vortex rings and vortex dipoles using vortex sheet methods. The author observed self-similar shedding of circulation into a tail in the roll-up of a spherical vortex sheet into a vortex ring, but no shedding of circulation in the roll-up of a cylindrical vortex sheet into a vortex pair.

Recently, Afanasyev (2006) and Pedrizzetti (2010) have considered the formation of two-dimensional dipoles by the ejection of fluid from thin slits. Unlike in the axisymmetric case, both studies found that vortex pairs continue to accept vorticity after ejection times well beyond those observed for circular vortex rings. Afanasyev (2006) also observed that, throughout their formation, vortex dipoles formed by the ejection of fluid from thin slits could be modelled by different members of a family of steadily translating vortex pairs described by Pierrehumbert (1980). These vortices form a family of constant-vorticity vortex pairs of finite core size, ranging from point vortex dipoles to the symmetry-axis-touching limit. Although the dipoles could be more realistically modelled by the more complex vorticity distributions proposed by Kizner & Khvoles (2004) and Khvoles, Berson & Kizner (2005), the Pierrehumbert family is of interest because of its simplicity, and because it serves as a two-dimensional analogue to the Norbury family of vortex rings.

In this study, we investigated the nonlinear perturbation response of the members of the families of vortices introduced by Norbury (1973) and Pierrehumbert (1980) to prolate shape perturbations similar to those considered by Pozrikidis (1986). The class of prolate perturbations considered was similar to that described in Pozrikidis (1986), yet differed slightly in its mathematical formulation due to geometrical constraints outlined in § 2.2. These perturbations are not of the circulation- and impulse-preserving type described by Benjamin (1976). However, they are of interest because the perturbations experienced by forming vortex rings and dipoles in an experimental setting are also not of the type described by Benjamin (1976). The response of the entire Norbury family to this type of perturbations was considered, in order to bridge the gap between the observations of Ye & Chu (1995) for thin-cored rings and those of Pozrikidis (1986) for Hill's spherical vortex. In particular, we searched for a change in the perturbation response as we considered vortex rings of increasing core thickness. Finally, we considered the difference in the responses of the Norbury and Pierrehumbert families, to ascertain whether they reflect the differences observed in the formation of vortices in axisymmetric and two-dimensional experiments.

Contour dynamics methods (Zabusky, Hughes & Roberts 1979; Shariff, Leonard & Ferziger 2008) were employed to compute the nonlinear evolution of members of the Norbury and Pierrehumbert families subject to prolate shape perturbations. We identified a change in the perturbation response of vortex rings as we considered members of the Norbury family with progressively thicker cores, and this change was found to be analogous to the onset of pinch-off in experimentally generated vortex rings. Furthermore, we found no such change in response when considering members of the Pierrehumbert family of increasing core size. This difference in behaviour between the two families is akin to the absence of a critical time scale in two-dimensional vortex dipole formation. We hypothesize that these findings on the perturbation response of low-order vortex models can be used to study and possibly predict pinch-off in real flows with more complex vorticity distributions.

The paper is organized as follows. In § 2 we introduce the mathematical formulation of the two vortex families, as well as the perturbation method and the contour dynamics procedures employed. This numerical method is employed in §§ 3 and 4 to examine the nonlinear evolution of perturbed members of the Norbury and Pierrehumbert families, respectively. Finally, concluding remarks are presented in § 5.

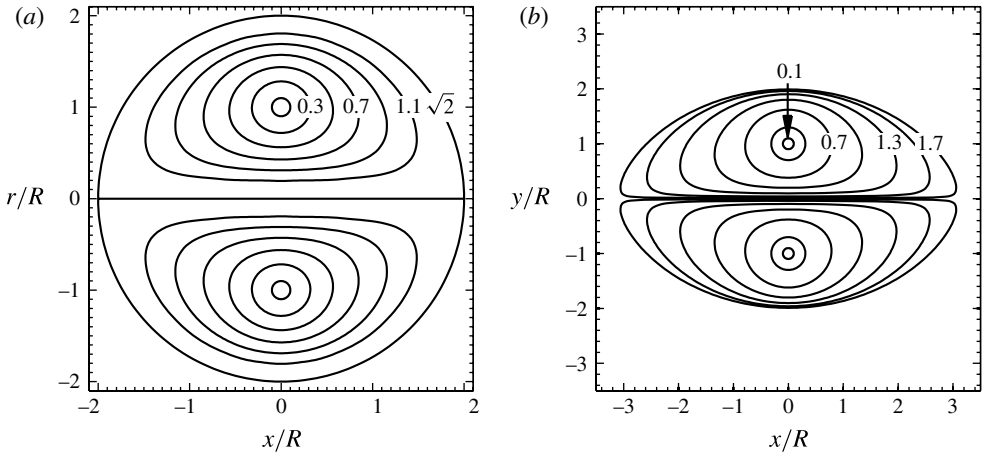

FIGURE 1. The Norbury (*a*) and Pierrehumbert (*b*) families of vortices. Core shapes for various values of α ranging from 0.2 to $\sqrt{2}$ (Norbury) and 0.1 to 1.7 (Pierrehumbert).

2. Mathematical formulation and numerical method

2.1. *The Norbury and Pierrehumbert families of solutions*

Norbury (1973) introduced a family of steadily translating solutions of the axisymmetric Euler equations, in the form of vortex rings with core boundary ∂A that satisfy:

$$\omega = \begin{cases} \Omega r & \text{inside } \partial A \\ 0 & \text{outside } \partial A \end{cases} \tag{2.1}$$

where Ω is a constant. He classified these rings by the parameter $\alpha = \sqrt{A/\pi R^2}$, where A is the core cross-sectional area and R is the ring radius (defined as the radial distance to the centre of the core). The parameter α is the ratio of the mean core radius to the ring radius, and it describes a family ranging from thin-cored vortex rings as α tends to zero, to Hill's spherical vortex for $\alpha = \sqrt{2}$. In figure 1(*a*), we present the calculated core boundary for Norbury vortices with various values of α, ranging from 0.2 to $\sqrt{2}$.

Similarly, Pierrehumbert (1980) found a steadily translating solution to the two-dimensional Euler equations, in the form of symmetric vortex pairs with boundary $\partial A_{1,2}$ that satisfy:

$$\omega = \begin{cases} \Omega & \text{inside } \partial A_1 \\ -\Omega & \text{inside } \partial A_2 \\ 0 & \text{elsewhere.} \end{cases} \tag{2.2}$$

Following Norbury (1973), the resulting family can also be parameterized by $\alpha = \sqrt{A/\pi R^2}$, where in this case R is defined as the distance from the symmetry axis to the centre of one of the symmetric vortices. The Pierrehumbert family spans the range from point-like vortices as $\alpha \to 0$, to symmetry-axis-touching vortex pairs. Figure 1(*b*) shows the calculated core boundaries $\partial A_{1,2}$ of Pierrehumbert pairs for values of α ranging from 0.1 to 1.7.

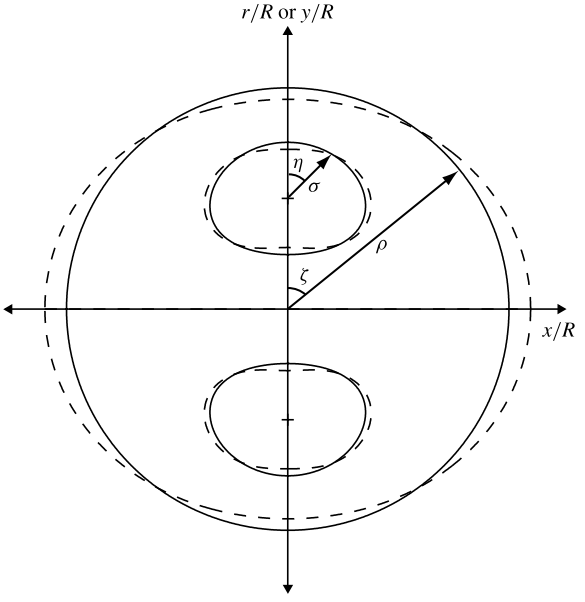

FIGURE 2. Perturbations and coordinates defined in the text. Hill's spherical vortex and a Norbury vortex with $\alpha = 0.6$ are depicted by the solid lines. The dashed lines represent a perturbation of $\epsilon = -0.1$ to Hill's spherical vortex, of the type studied by Pozrikidis (1986), as well as a perturbation to the Norbury vortex of $\delta = -0.1$ as defined in (2.5). The vortices propagate from left to right.

The shapes of the members of the Norbury family were determined using the numerical method outlined in Norbury (1973), which required solving the integral equation for the streamfunction using a modified Newton–Raphson method. Similarly, the shapes of the members of the Pierrehumbert family were determined by solving the corresponding integral equation for the streamfunction using the relaxation method described in Pierrehumbert (1980). Note that the symmetry-axis-touching solution is not depicted in figure 1(*b*). Pierrehumbert (1980) found an axis-touching solution which included a cusp at the symmetry axis. Shortly thereafter, Saffman & Tanveer (1982) demonstrated that the axis-touching solution is not unique, and presented an alternative solution with no cusp. However, whether this solution is the limiting case for the Pierrehumbert family remains an open question (Saffman & Szeto 1980). In this study, we have excluded the axis-touching case from the analysis for simplicity.

2.2. *Shape perturbations*

Pozrikidis (1986) studied the response of a limiting member of the Norbury family, namely a Hill's spherical vortex of radius $2R$, to prolate and oblate shape perturbations. He introduced the spheroidal perturbations by expressing the boundary of the vortex in the form:

$$\rho = 2R\gamma \left(1 + \frac{\epsilon}{4}(1 + 3\cos 2\zeta)\right) \tag{2.3}$$

where ρ and ζ are, respectively, the vortex radius and polar angle defined in figure 2. The spheroidal perturbations were achieved by introducing a perturbed second-order Fourier mode, which was scaled by a fraction of the unperturbed vortex radius,

$(3\epsilon/2)R$, to the expression for the vortex core boundary. The sign of the parameter ϵ indicates the direction of the deviation from the spherical shape, with a positive value corresponding to an oblate perturbation and a negative value corresponding to a prolate perturbation. The factor $\gamma(\epsilon)$ was introduced to preserve the original vortex core circulation, implying that the perturbations constitute rearrangements of the vorticity density.

In the formulation of Pozrikidis (1986), the vortex radius and polar angle were measured from the centre of the spherical vortex, which is on the symmetry axis of the flow. In the more general case of the Norbury and Pierrehumbert families, however, such a formulation is not possible, as the vortex cores are not symmetry-axis-touching in general. As a result, the core boundary for each member of the Norbury and Pierrehumbert families is defined here in polar coordinates measured from the centre of the core. In this coordinate system, the core boundary ∂A can be expressed in the form of a Fourier cosine polynomial:

$$\sigma = f(\eta, \alpha) = \sum_{j=0}^{N} a_n(\alpha) \cos j\eta \tag{2.4}$$

where N was chosen to be 30, and the quantities σ and η (defined in figure 2) are the local core radius and the polar angle measured from the centre of the core, respectively. In this formulation, perturbations to the core boundary similar to those first introduced to circular vortex patches by Kelvin (1880*a*) can be readily introduced. Following Pozrikidis (1986), we introduced shape perturbations to ∂A by adding a fraction of the mean core radius ($\delta\alpha R$) to the second-order mode:

$$\sigma = f(\eta, \alpha) = \gamma \sum_{j=0}^{N} a'_n(\alpha) \cos j\eta, \tag{2.5}$$

$$a'_2 = a_2 + \delta\alpha R, \tag{2.6}$$

$$a'_j = a_j \quad \text{for } j \neq 2; \tag{2.7}$$

δ expresses the deviation from the unperturbed shape, and it takes positive values for oblate perturbations and negative values for prolate perturbations. For consistency with the previous studies by Pozrikidis (1986) and Ye & Chu (1995), the factor $\gamma(\alpha, \delta)$ was introduced in order to preserve the unperturbed core circulation. For each member of the family and perturbation size δ analytical expressions for the circulation of the perturbed and unperturbed vortices were obtained by integrating the vorticity over the regions described by (2.4) and (2.5)–(2.7). To meet the requirement that the circulation remain unchanged, these two expressions were equated and the value of the multiplicative constant $\gamma(\alpha, \delta)$ was determined by solving the resultant cubic equation.

Like the perturbations introduced by Pozrikidis (1986), these perturbations constitute rearrangements of the unperturbed vorticity. However, both types of perturbations differ from those described by Benjamin (1976) in that the perturbed vortices do not preserve the unperturbed vortex impulse. These perturbations are of interest because the perturbations encountered by vortex rings and dipoles in an experimental setting are also not of the impulse- and circulation-preserving type described by Benjamin (1976). Furthermore, the fact that, in his study of Hill's vortex, Pozrikidis (1986) reported a detrainment of circulation analogous to pinch-off utilizing these types of perturbations suggests that they are suited for the study of an analogue to pinch-off in the Norbury and Pierrehumbert families.

The perturbations described in (2.5)–(2.7) differ from those described in (2.3), in that Pozrikidis perturbed only the shape of the outer boundary of the vortex core (a semi-circle of radius $2R$) while scaling the portion of the boundary nearest the symmetry axis (for Hill's spherical vortex, a straight line at the symmetry axis), in order to preserve the continuity of the core boundary. In contrast, our formulation results in a perturbation being introduced to the entire core boundary. As a result, for Hill's spherical vortex, our perturbation is not equivalent to the type of perturbations considered by Pozrikidis (1986). Hence, the perturbation scheme described in (2.3) was employed in validating our implementation of the numerical method described in the following section against the results of Pozrikidis (1986) (§ 2.5). Subsequently, however, the perturbations described in (2.5)–(2.7) were applied in order to investigate the nonlinear perturbation response of the Norbury and Pierrehumbert families.

2.3. *Contour dynamics formulation*

The evolution of the perturbed vortex cores was computed using contour dynamics methods. The original two-dimensional contour dynamics solution is due to Zabusky *et al.* (1979); however, we employed an alternative formulation from Pullin (1991). The velocity induced by one of the symmetric vortex patches in a Pierrehumbert pair at a point $z = x + \mathrm{i}y$ in the complex plane was computed using:

$$u_x + \mathrm{i}u_y = -\frac{\Omega}{4\pi}\oint_{\partial A} \frac{z - z'}{\bar{z} - \bar{z}'}\,\mathrm{d}z'. \tag{2.8}$$

Shariff *et al.* (2008) extended the contour dynamics method to the case of axisymmetric vortex rings with a linear vorticity distribution in the radial direction, such as the Norbury family. In this case, the velocity induced by a compact region of vorticity A at a point $\boldsymbol{x}$ is given by:

$$\boldsymbol{u}(\boldsymbol{x}) = \Omega \oint_{\partial A} [(x - x')G(s')\cos\theta' - rH(s')\sin\theta']\,\hat{x} + r'H(s')\cos\theta'\hat{r}\,\mathrm{d}s', \tag{2.9}$$

$$G(s') = \frac{r'}{\pi\sqrt{A + B}}K(k), \tag{2.10}$$

$$H(s') = \frac{1}{2\pi r}\left(\frac{A}{\sqrt{A + B}}K(k) - E(k)\sqrt{A + B}\right), \tag{2.11}$$

$$k = \sqrt{\frac{2B}{A + B}}, \tag{2.12}$$

$$A = (x - x')^2 + r^2 + r'^2, \quad B = 2rr', \tag{2.13}$$

where $\theta(t, \alpha)$ is the angle of the outward-pointing normal relative to the symmetry axis, and $K(k)$ and $E(k)$ are the complete elliptic integrals of the first and second kind, respectively.

2.4. *Numerical method*

The contour dynamics formulation reduces the evolution problem to tracking the motion of a collection of marker points on the core boundary by numerical integration of (2.8) or (2.9). Contour integration was performed by discretizing the boundary using linear segments, and evaluating the contribution from segments not adjacent to the field point using Gaussian quadrature. The singularities in the evolution equations were dealt with by explicit evaluation in the two-dimensional case, and using the method outlined by Shariff *et al.* (2008) in the axisymmetric case.

The solution was marched forward in time using a fourth-order Runge–Kutta scheme. At each time step, additional marker points were inserted where the linear segments stretched beyond $0.016R$, and removed where segments shrunk below $0.004R$ (Shariff *et al.* 2008). Following Shariff *et al.* (2008), the time step was chosen to satisfy $\Delta T = 0.05/\Omega_0$, where Ω_0 is the vorticity at the centre of the vortex ring core in the axisymmetric case ($\Omega_0 = \Omega R$), or the strength of the positively signed vortex patch in the two-dimensional case. The flow invariants (circulation, impulse, and energy) were monitored and their change was kept below 0.01 % over one eddy turnover period for the impulse and circulation, and 0.02 % over the same period for the energy.

2.5. *Verification*

In order to validate our implementation of the numerical algorithms described in the preceding section, we began by considering the response of Hill's spherical vortex to spheroidal shape perturbations of the type investigated by Pozrikidis (1986) and described in (2.3). Figure 3 illustrates the response of Hill's spherical vortex to a small-amplitude prolate perturbation with $\epsilon = -0.05$. The perturbed vortex is seen to detrain rotational fluid into a vortex tail (figure 3*c*), which experiences continual elongation (figure 3*d*) and tends to form an independent low-circulation entity which trails behind the ring (figure 3*e*). As noted by Gharib *et al.* (1998), the shedding of rotational fluid into a vortex tail is akin to the pinch-off phenomenon observed in experimentally generated vortex rings.

The results presented in figure 3 agree qualitatively with the results of Pozrikidis (1986) for a spherical vortex subjected to the same perturbation, and computed using a different contour dynamics formulation and numerical scheme (cf. figure 2 in Pozrikidis 1986). In figure 4(*a*) we present the deviation of the non-dimensional vorticity centroid location from its unperturbed equivalent ($x_c^* = (Ut - x_c)/R$, defined in Pozrikidis 1986) as a function of non-dimensional time $t^* = Ut/R$, where U is the translational speed of the unperturbed spherical vortex. The lines indicate the present results for vortices subjected to perturbations of $\epsilon = -0.05$, $\epsilon = -0.15$, and $\epsilon = -0.3$, and the symbols indicate the results of Pozrikidis (1986) for the same perturbations. Similarly, figure 4(*b*) shows the present measurements of the time evolution of the vortex speed ($U_c^* = \mathrm{d}x_c^*/\mathrm{d}t^*$) for the same three perturbation sizes, as well as those of Pozrikidis (1986). In both figures 4(*a*) and 4(*b*), the agreement with Pozrikidis (1986) is found to be excellent.

3. Response of the Norbury family of vortex rings

Having validated our implementation of the numerical method described in § 2.4, we considered the response of the remaining members of the Norbury family to shape perturbations of the type described in (2.5)–(2.7). Pozrikidis (1986) reported detrainment of circulation into a vortex tail only for prolate shape perturbations, a phenomenon of interest because it is analogous to pinch-off. Therefore, we limited our study to the response of the remainder of the family to prolate perturbations, with the goal of characterizing the response of the entire Norbury family and investigating the extent of the shedding behaviour. We simulated the evolution of members of the Norbury family with α ranging from 0.2 to 1.2, subject to prolate perturbations with $\delta = -0.01$, $\delta = -0.02$ and $\delta = -0.05$.

Figures 5 to 7 show the evolution of different Norbury vortices subjected to a perturbation of 5 % of the mean core radius ($\delta = -0.05$). Thin-cored members of

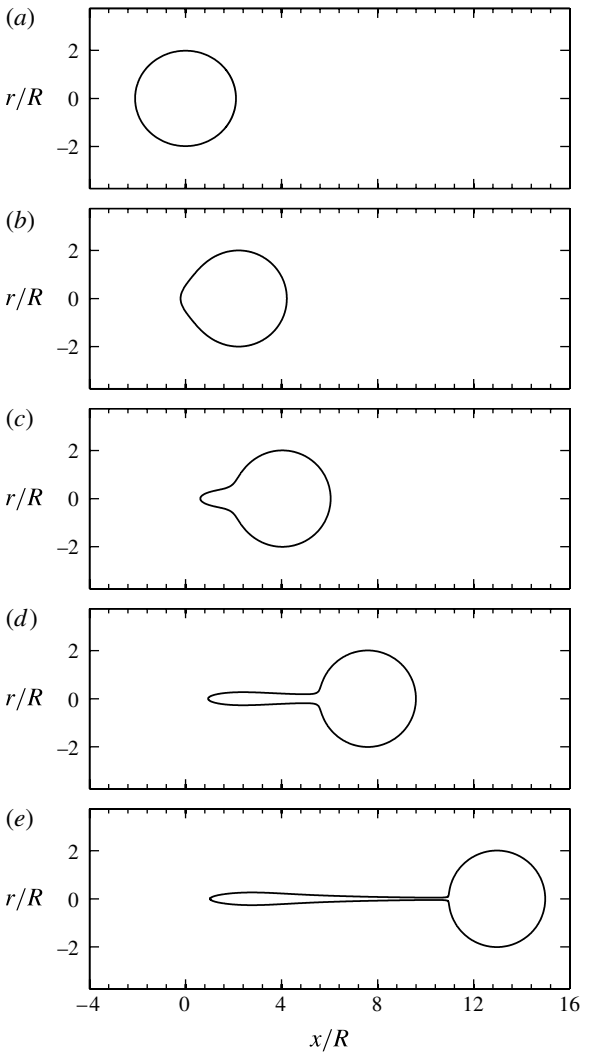

FIGURE 3. Evolution of Hill's spherical vortex subject to a Pozrikidis perturbation with $\epsilon = -0.05$ at: (*a*) $t^* = 0$; (*b*) $t^* = 2.1$; (*c*) $t^* = 4.0$; (*d*) $t^* = 7.4$; (*e*) $t^* = 12.8$.

the family ($\alpha < 0.7$) were found to propagate along the axial direction whilst their vortex cores underwent a quasi-periodic deformation. Eventually, the formation of small mounds on the core boundary led to the development of thin filaments, which wrapped around the vortex core. The filamentation of the vortex is a common feature in vortex dynamics, and it is observed even in linearly stable configurations (Deem & Zabusky 1978; Dritschel 1988*a*,*b*; Saffman 1992; Crowdy & Surana 2007). Thus, Pozrikidis (1986) and Ye & Chu (1995) remark that the appearance of thin filaments is of negligible importance to the dynamics of the perturbed vortex. Figure 5 depicts the evolution of a Norbury vortex with $\alpha = 0.5$ subject to a perturbation of $\delta = -0.05$. Initially, the vortex core was found to undergo a quasi-periodic shape deformation (figure 5*a*–*c*). The small deformation which was initially seen to propagate along the

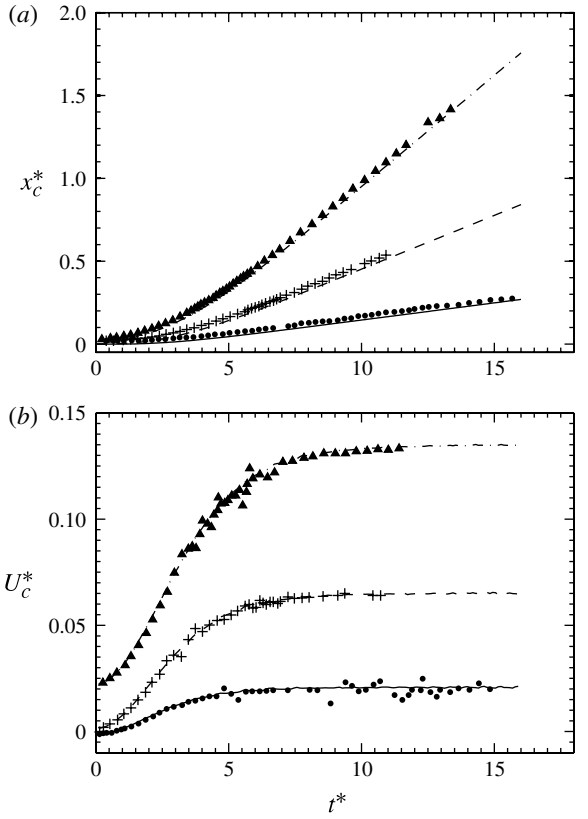

FIGURE 4. Evolution of (*a*) the deviation of the vorticity centroid from the unperturbed centroid ($x_c^* = (Ut - x_c)/R$) and (*b*) the vortex speed $U_c^* = \mathrm{d}x_c^*/\mathrm{d}t^*$ for prolate Pozrikidis perturbations. The symbols show the results of Pozrikidis (1986) for: •, $\epsilon = -0.05$; +, $\epsilon = -0.15$; ▲, $\epsilon = -0.3$. The lines show our results for the same perturbations: —, $\epsilon = -0.05$; – –, $\epsilon = -0.15$; –·–; $\epsilon = -0.3$.

contour (figure 5*b*,*c*), eventually sharpened into a corner (figure 5*d*) and developed into a thin filament by $t^* = Ut/R = 6.75$ (figure 5*e*).

For members of the Norbury family with increasing core thickness, the core cross-section increasingly resembled a semi-circle, and the curvature of the portion of the boundary closest to the symmetry axis approached zero. The perturbation scheme outlined in (2.5)–(2.7) therefore resulted in a perturbed vortex shape that was locally concave (see figure 2). As these vortices evolved, the region of concavity propagated along the contour, due to the motion of the rotational fluid within. Once the region of concavity reached the corner near the front of the vortex, it led to the formation of a small mound on the contour, which rapidly developed into a vortex filament. The filamentation of a sufficiently perturbed vortex has been observed consistently in previous studies (Deem & Zabusky 1978; Dritschel 1988*a*,*b*; Saffman 1992; Crowdy & Surana 2007), and as such the emission of a filament by these perturbed Norbury vortices is to be expected. What is particular to these vortices is the development of the filament consistently at the location of the region of initial concavity, by the mechanism described above.

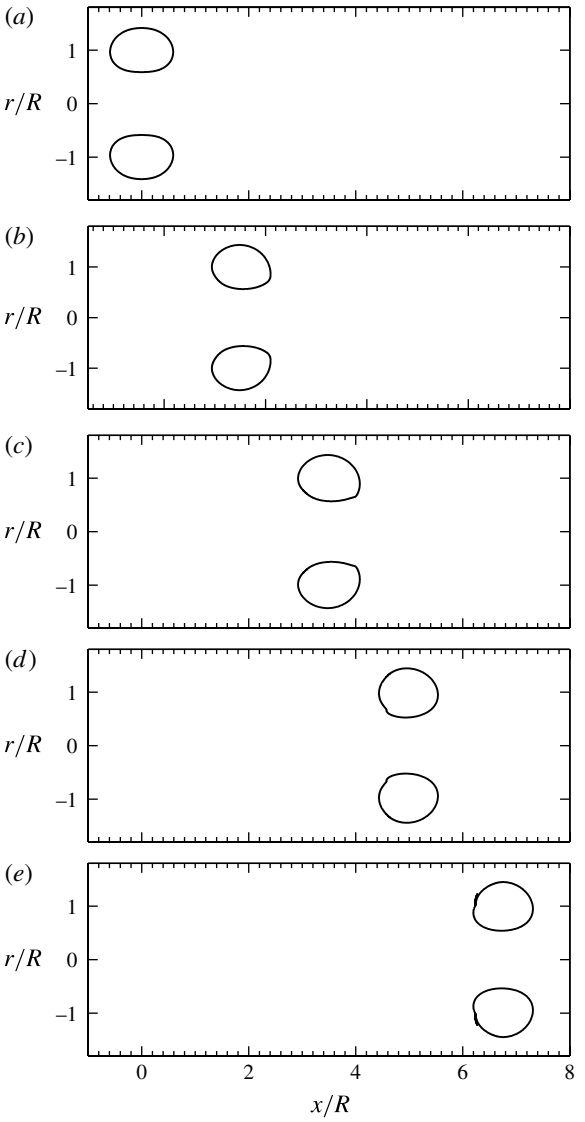

FIGURE 5. Evolution of a Norbury vortex with $\alpha = 0.5$ subject to a prolate perturbation of $\delta = -0.05$ at: (*a*) $t^* = 0$; (*b*) $t^* = 1.5$; (*c*) $t^* = 3.5$; (*d*) $t^* = 5$; (*e*) $t^* = 6.75$.

Figure 6 depicts the behaviour typical of Norbury vortices with $0.7 < \alpha < 0.95$, when subjected to a perturbation of $\delta = -0.05$. In figure 6(*a*), a perturbed Norbury vortex with $\alpha = 0.9$ exhibits a region of local concavity on the portion of its boundary nearest the symmetry axis of the ring. A small mound was seen to develop as the region of concavity reached the front of the vortex, which by $t^* = 2.5$ had developed into a sharp spike (figure 6*b*). At later times, this spike was seen to develop into a thin filament which wrapped around the vortex core (figure 6*c–e*). The filament increased in length as the simulation progressed; however no detrainment of circulation into a trailing vortex tail was observed. These results are in good qualitative agreement with

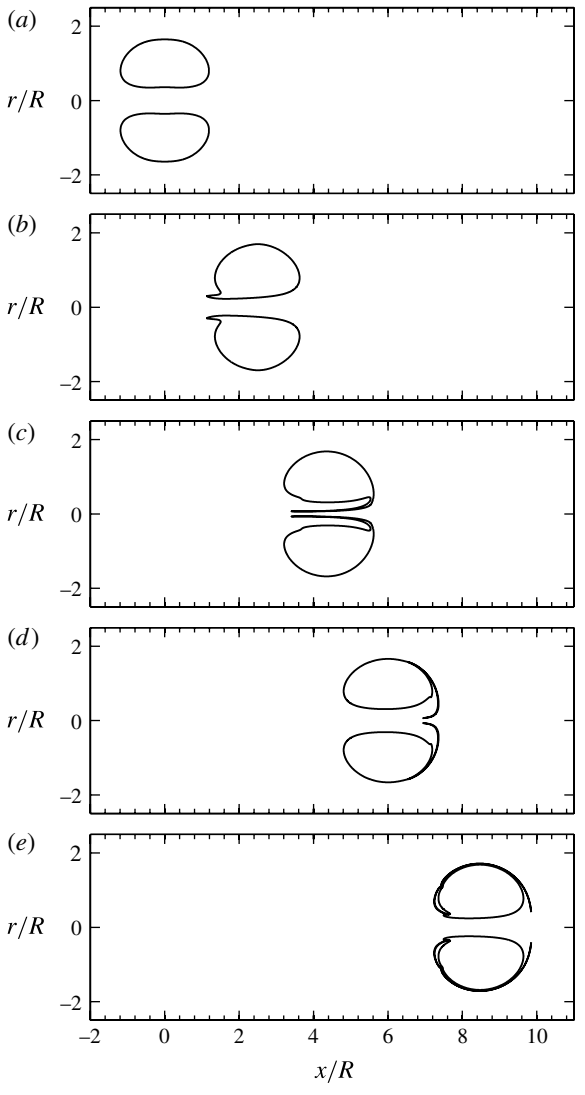

FIGURE 6. Evolution of a Norbury vortex with $\alpha = 0.9$ subject to a prolate perturbation of $\delta = -0.05$ at: (*a*) $t^* = 0$; (*b*) $t^* = 2.5$; (*c*) $t^* = 4.5$; (*d*) $t^* = 6$; (*e*) $t^* = 8.5$.

those of Ye & Chu (1995), who considered the unsteady evolution of a Norbury vortex with $\alpha = 0.8$, subject to a perturbation of $\delta = -0.15$.

However, for thicker-cored members of the family subject to perturbations of the same size, a change in response was observed. For Norbury vortices with $\alpha > 0.95$, the introduction of a prolate perturbation with $\delta = -0.05$ resulted in the detrainment of rotational fluid into a vortex tail which lingered behind the vortex ring. Figure 7 shows the evolution of a Norbury vortex with $\alpha = 1.2$ subject to a perturbation of this magnitude. Initially, excess rotational fluid from the outer regions of the core was convected towards the rear of the vortex (figure 7*b*). Figure 7(*c–e*) depicts the elongation of this region of accumulated vorticity, under the influence of the high-strain region near the rear stagnation point, into a long tail which lingered behind

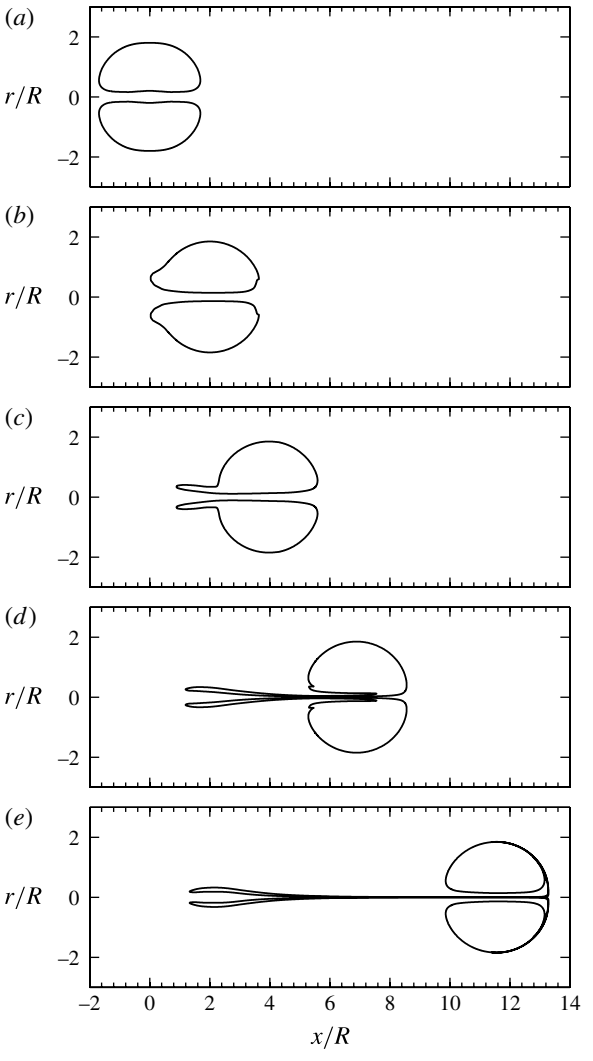

FIGURE 7. Evolution of a Norbury vortex with $\alpha = 1.2$ subject to a prolate perturbation of $\delta = -0.05$ at: (*a*) $t^* = 0$; (*b*) $t^* = 2$; (*c*) $t^* = 4$; (*d*) $t^* = 7$; (*e*) $t^* = 11.7$.

the vortex ring and formed an independent low-circulation entity. These observations are consistent with the results of Pozrikidis (1986) for the evolution of Hill's spherical vortex under similar shape perturbations, as well as with the observations of Gharib *et al.* (1998) for experimentally generated vortex rings above a formation time of $T^* = 4$.

In comparing the shedding of a vortex tail by a perturbed Hill's vortex and the phenomenon of pinch-off, Gharib *et al.* (1998) found that the processes are analogous, since both occur when patches of rotational fluid at the outer regions of the core are no longer contained within the region of fluid translating with the vortex ring and are hence convected to the rear of the vortex. In doing so, the excess rotational fluid enters the high-strain region near the rear stagnation point and is elongated under the influence of the stagnation-point flow to form a vortex tail. In nearly spherical

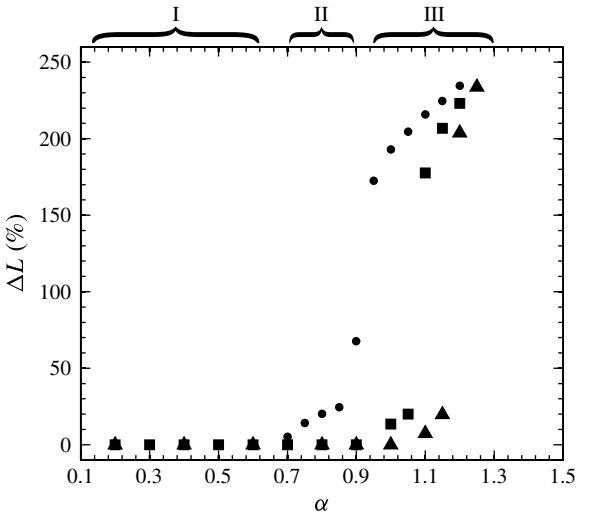

FIGURE 8. Contour length of the tail or filament after one eddy turnover (expressed as a percentage of the initial contour length) for members of the Norbury family subject to perturbations of different magnitudes: ▲, $\delta = -0.01$; ■, $\delta = -0.02$; ●, $\delta = -0.05$.

members of the Norbury family, the boundary of the vortex core lies close to the stagnation streamline. Consequently, a large enough shape perturbation was found to lead to the presence of excess rotational fluid in the region where fluid particles were being swept past the ring. The excess vorticity was hence convected to the rear of the vortex, where the proximity of the rear stagnation point resulted in its detrainment into a tail. In contrast, for thin-cored members of the Norbury family, the excess vorticity was found to revolve around the vortex core and eventually cause filamentation, but it was not detrained due to the remoteness of the rear stagnation point.

A simple metric for comparing the response of the different members of the family is the contour length of the vortex tail or filament after one eddy turnover (ΔL), expressed as a percentage of the initial contour length. In figure 8 we present the contour length (ΔL) as a function of the parameter α for three different perturbation sizes: $\delta = -0.05$, $\delta = -0.02$, and $\delta = -0.01$. The results for $\delta = -0.05$ form a curve with three distinct sections, labelled I, II and III in figure 8. For small values of α, the change in the contour length is negligible, since these thin-cored rings were found to undergo quasi-periodic deformations for several eddy turnovers before thin filaments began to develop (region I). For values of α in the 0.7–0.95 range, ΔL increases with increasing core thickness (region II). This region corresponds to the members of the family for which a perturbation of this magnitude results in an initial core shape which exhibits regions of local concavity. For these vortices, thin filaments were found to develop immediately, and result in a finite ΔL after one eddy turnover.

The most salient feature of the curve, however, is the sharp increase in contour length when the core thickness parameter is increased past $\alpha = 0.95$ (region III). This discontinuity coincides with the first instance of tail shedding in the family, and is indicative of a change in the response of the Norbury family to perturbations of this size. The sharp increase in ΔL is also evident in the results for $\delta = -0.02$ and $\delta = -0.01$, shown in figure 8, and it was also found to coincide with the onset of trailing vortex tail formation for perturbations of these sizes. Notably, the value of α

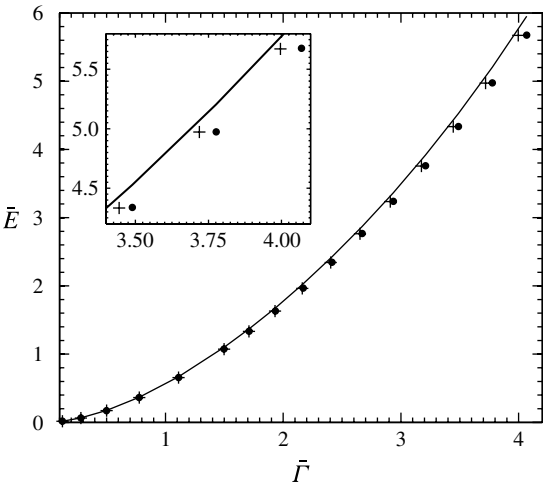

FIGURE 9. Kinetic energy ($\bar{E}$) versus circulation ($\bar{\Gamma}$) for Norbury vortices subject to a perturbation of $\delta = -0.05$. The solid line shows the $\bar{\Gamma}$–$\bar{E}$ curve for the unperturbed Norbury family. The filled dots represent the initial circulation and energy of the perturbed vortices. The crosses represent the values that the perturbed vortices asymptote to after contour surgery. The same quantities are shown on the inset, which focuses on the thick-cored members of the family.

at which the detrainment of circulation into a tail was first observed appeared to be dependent on the perturbation size.

In the preceding figures, contour surgery (Dritschel 1988*a*) was not applied, and the filaments and vortex tails were allowed to grow, in order to observe the initial development of the instability. By excizing the vortex filaments, however, we observed the development of the perturbed vortices into nearly steady vortex rings whose asymptotic shape was another member of the Norbury family. Figure 9 shows the non-dimensional kinetic energy ($\bar{E} = E/(\rho\Omega^2 R^7)$) as a function of the non-dimensional circulation ($\bar{\Gamma} = \Gamma/(\Omega R^3)$), for steadily translating and perturbed members of the Norbury family. The solid line depicts the $\bar{\Gamma}$–$\bar{E}$ curve for the unperturbed members of the Norbury family, while the black dots represent the initial circulation and energy of the perturbed vortices ($\delta = -0.05$), and the crosses represent the asymptotic states. Since the perturbations are circulation-preserving, the perturbed vortices are shifted downwards from the unperturbed curve by an amount $\Delta\bar{E}(\alpha)$, which is greater for thicker-cored members of the family. The perturbed vortices in regions I and II were found to lose small amounts of both energy and circulation through filamentation, as their shape slowly approached a nearly steady state with a slightly smaller mean core radius than they originally possessed. In contrast, in detraining circulation into a vortex tail, the vortices in region III rapidly shed circulation and a comparatively small amount of kinetic energy. This resulted in a near-horizontal shift in the $\bar{\Gamma}$–$\bar{E}$ curve, as shown in figure 9. After the initial detrainment, these vortices continued to approach a steady state by successively losing small amounts of circulation and energy by filamentation, much like the vortices in regions I and II.

The nonlinear response of the Norbury family to arbitrary shape perturbations intended to resemble those encountered by experimentally generated vortex rings (such as adding a 'tail' of vorticity to the rear of a Norbury vortex) was also considered.

For these perturbations, the results were qualitatively similar to those reported above for prolate shape perturbations, with thick-cored members of the family exhibiting detrainment of circulation, and thinner-cored members displaying only filamentation. However, these arbitrary shape perturbations proved difficult to quantify due to the absence of conserved quantities, and thus an accurate comparison between different members of the Norbury family and across families was not possible. As a result, the aforementioned prolate shape perturbations were selected for this study.

4. Response of the Pierrehumbert family of vortex pairs

Unlike that of the Norbury family, the stability of the Pierrehumbert family has been the subject of numerous contour dynamics studies. Dritschel (1995) examined the linear stability of the family of dipoles, and used contour dynamics to find the nonlinear stability bounds for asymmetric perturbations. Recently, Makarov & Kizner (2011) used contour dynamics methods to show that all members of the Pierrehumbert family are stable with respect to symmetric perturbations. However, the nonlinear response of this family to prolate perturbations of the type described in § 2 has not been previously reported. Since a comparison between the perturbation responses of the two families is instructive, we considered the response of several members of the Pierrehumbert family to perturbations of the same kind and size as those introduced to the Norbury family.

Given the recent results of Makarov & Kizner (2011) it is unsurprising that, in the case of the Pierrehumbert family, we found no evidence of detrainment of rotational fluid into a trailing vortex tail, even when thick-cored members of the family were subjected to the largest of the perturbations considered ($\delta = -0.05$). Figure 10 depicts the evolution of a Pierrehumbert vortex pair with $\alpha = 1.2$ under a perturbation of $\delta = -0.05$. The cores of the vortices in this pair are quite thick, yet the pair's behaviour resembled that of the thin-cored Norbury vortex depicted in figure 5. The vortex cores were observed to undergo quasi-periodic shape deformations, and thin filaments eventually began to form where the perturbed cores were locally concave.

Figure 11 shows a plot of the excess energy as a function of circulation for the unperturbed Pierrehumbert family (solid line), and for the initial and asymptotic states of the members of this family subject to shape perturbations with $\delta = -0.05$ (filled circles and crosses, respectively). It is interesting to note that, in the case of the Pierrehumbert family, symmetric perturbations of the same type and size as those introduced to the Norbury family result in very small changes in the excess energy of the dipoles. Whereas for the Norbury family, perturbations with $\delta = -0.05$ resulted in decreases in the kinetic energy of the perturbed vortex of up to 4.5 %, in this case the change was found to be less than 0.3 %. Furthermore, it was found that producing percentage decreases in the energy of the order of those observed for the Norbury family required introducing perturbations so extreme that the perturbed vortices resembled figure-eights. This robustness of the energy to shape perturbations leads to the observed absence of tail shedding.

5. Conclusions

The nonlinear response of the Norbury family of axisymmetric vortex rings to prolate shape perturbations has been considered. Our contour dynamics computations suggest that, for prolate shape perturbations, there is a dynamical change in the perturbation response as we traverse the Norbury family from thin-cored members to thicker-cored vortex rings, which is analogous to the onset of pinch-off in

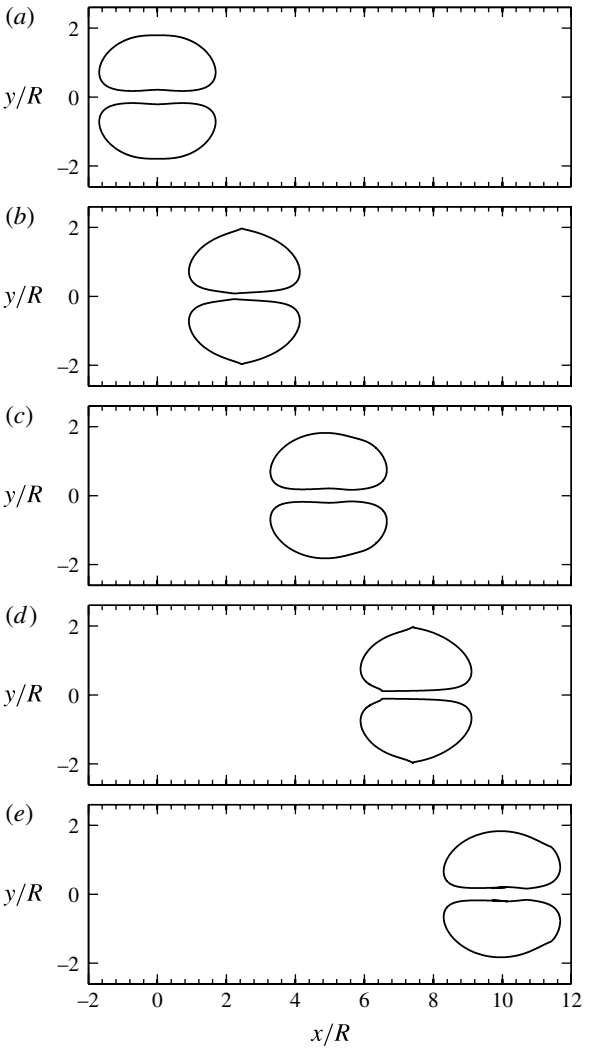

FIGURE 10. Evolution of a Pierrehumbert vortex with $\alpha = 1.2$ subject to a prolate perturbation of $\delta = -0.05$ at: (*a*) $t^* = 0$; (*b*) $t^* = 2.5$; (*c*) $t^* = 5$; (*d*) $t^* = 7.5$; (*e*) $t^* = 10$.

experimentally generated vortex rings. Thin-cored vortex rings were found to undergo quasi-periodic shape deformations, and to eventually develop thin filaments which are largely dynamically unimportant. In contrast, in thick-cored vortex rings we observed the transport of excess rotational fluid from the outer boundaries of the core to the rear of the vortex, which led to the development of a trailing vortex tail and the detrainment of circulation into a separate trailing entity.

While the behaviour of Hill's spherical vortex and of one thin-cored member of the family under similar conditions has been previously reported, the present results illustrate the behaviour of the entire family in a manner consistent with the results of Pozrikidis (1986) and Ye & Chu (1995) for these two special cases. Furthermore, the change in response observed as we traversed the Norbury family is consistent with experimental observations of the formation of circular vortex rings. Thick-cored

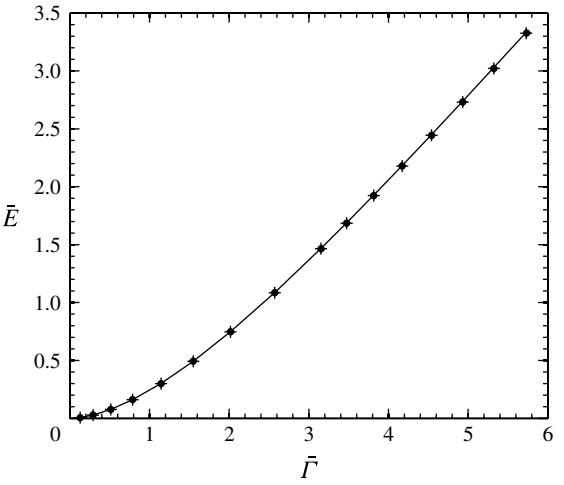

FIGURE 11. Excess kinetic energy ($\bar{E} = E/(\rho\Omega^2 R^4)$) versus circulation ($\bar{\Gamma} = \Gamma/(\Omega R^2)$) for Pierrehumbert vortices subject to a perturbation of $\delta = -0.05$. The solid line shows the $\bar{\Gamma}$–$\bar{E}$ curve for the unperturbed Pierrehumbert family. The filled dots represent the initial circulation and energy of the perturbed vortices. The crosses represent the values that the perturbed vortices asymptote to after contour surgery.

vortex rings have been shown to detrain excess vorticity into a trailing jet in numerous experiments (Gharib *et al.* 1998; Dabiri & Gharib 2004; Krueger, Dabiri & Gharib 2006; Pawlak *et al.* 2007). As Gharib *et al.* (1998) remark, this process is analogous to the detrainment of circulation into a tail by thick-cored members of the Norbury family observed in this study.

In contrast, we found no evidence of detrainment of circulation or tail shedding for members of the Pierrehumbert family of all core sizes subject to equivalent perturbations. This suggests a difference in the perturbation response of the two-dimensional family compared to the axisymmetric Norbury family, which is attributed to the insensitivity of the kinetic energy of the Pierrehumbert dipoles to shape perturbations of the type considered (figure 11). This difference in response is of interest because it mirrors the observed differences in the vortex formation processes in the two-dimensional and axisymmetric configurations. Recent studies by Nitsche (2001), Afanasyev (2006) and Pedrizzetti (2010) suggest that the limiting time scale for axisymmetric vortex ring formation does not apply to the formation of two-dimensional vortex dipoles. In the light of our findings for the Norbury family, the absence of tail shedding for any members of the Pierrehumbert family is in good agreement with these studies.

The present results show that only instantaneous shape perturbations to low-order vortex patch models are required to produce a change in response between thin-cored vortex rings and thicker-cored rings which is consistent with experimental results, whereas no such transition is evident in vortex dipoles of any size. This is of particular interest given that the Norbury family has been successfully employed to model the growth of experimental vortex rings (Gharib *et al.* 1998; Mohseni & Gharib 1998; Shusser & Gharib 2000; Linden & Turner 2001), and that Afanasyev (2006) has noted that vortex dipoles closely resemble members of the Pierrehumbert family during their development.

In reality, however, vortex rings and dipoles formed from roll-up of a shear layer exhibit a Gaussian vorticity distribution and are subject to a continuous injection of vorticity from the shear layer. A more realistic vorticity distribution within the vortex cores could be achieved by employing nested contours. In addition, more realistic, continuous vortex models are available (Boyd & Ma 1990; Khvoles *et al.* 2005; Albrecht 2011), as are the viscous numerical methods necessary to study the perturbation response of such vortices. Although more computationally expensive, further work employing more realistic vorticity distributions, and analysing the response to perturbations where vorticity is continuously injected at the rear of the vortex, could yield further insight into the dynamics of the pinch-off of vortex rings from their feeding shear layer.

The results of this study suggest the existence of a relationship between vortex formation and the perturbation response of the leading vortex in a starting jet, which allows for the possibility of predicting pinch-off based on the properties of the developing vortex ring. Experimentally generated vortex rings can be characterized by their non-dimensional circulation and energy to construct circulation-energy diagrams such as those presented in §§ 3 and 4. Hence, the point on the $\bar{\Gamma}$–$\bar{E}$ diagram corresponding to the onset of pinch-off can be identified. If pinch-off is modelled as the point at which prolate perturbations to the leading vortex ring of a characteristic size lead to the detrainment of circulation, then the characteristic perturbation size can be determined by finding the perturbation size at which detrainment of circulation is first observed at the point on the $\bar{\Gamma}$–$\bar{E}$ diagram corresponding to pinch-off. Thus, the core thickness α at which pinch-off is expected to occur under a variety of conditions can be determined, and subsequently pinch-off can be predicted by considering only the characteristics of the leading vortex ring.

Such a perturbation-response-based criterion has the advantage that it could potentially be extended even to non-axisymmetric vortex rings, and could thus prove useful in a variety of biological applications where asymmetric vortex rings are the norm. Examples include the wakes of swimming and flying animals (Dickinson & Götz 1996; Kern & Koumoutsakos 2006; Kim & Gharib 2011) and the flow through the mitral valve in the human heart (Bellhouse 1972; Reul, Talukder & Muller 1981; Wieting & Stripling 1984; Domenichini, Pedrizzetti & Baccani 2005).

Acknowledgements

This work was funded by an NSF Graduate Research Fellowship to C.O'F., and by Office of Naval Research awards N000140810918 and N000141010137 to J.O.D. The authors would like to thank Professor T. Leonard for the many helpful discussions on the axisymmetric contour dynamics formulation.

REFERENCES

AFANASYEV, Y. D. 2006 Formation of vortex dipoles. *Phys. Fluids* **18**, 037103.

ALBRECHT, T. R. 2011 Steady vortex dipoles with general profile functions. *J. Fluid Mech.* **670**, 85–95.

BELLHOUSE, B. J. 1972 Fluid mechanics of a model mitral valve and left ventricle. *Cardiovascular Res.* **6**, 199–210.

BENJAMIN, T. B. 1976 The alliance of practical and analytical insights into the nonlinear problems of fluid mechanics. In *Applications of Methods of Functional Analysis to Problems in Mechanics* (ed. P. Germain & B. Nayroles), pp. 8–28. Springer.

BOYD, J. P. & MA, H. 1990 Numerical study of elliptical modons using a spectral method. *J. Fluid Mech.* **221**, 597–611.

COUDER, Y. & BASDEVANT, C. 1986 Experimental and numerical study of vortex couple in two-dimensional flows. *J. Fluid Mech.* **173**, 225–251.

CROWDY, D. & SURANA, A. 2007 Contour dynamics in complex domains. *J. Fluid Mech.* **593**, 235–254.

DABIRI, J. O. & GHARIB, M. 2004 Delay of vortex ring pinch-off by an imposed bulk counterflow. *Phys. Fluids* **16** (L), 28–30.

DEEM, G. S. & ZABUSKY, N. J. 1978 Vortex waves: stationary 'V states', interactions, recurrence and breaking. *Phys. Rev. Lett.* **40**, 859–862.

DICKINSON, M. H. & GÖTZ, K. G. 1996 The wake dynamics and fly forces of the fruit fly *Drosophila melanogaster*. *J. Expl Biol.* **199**, 2085–2104.

DOMENICHINI, F., PEDRIZZETTI, G. & BACCANI, B. 2005 Three-dimensional filling flow into a model left ventricle. *J. Fluid Mech.* **539**, 179–198.

DRITSCHEL, D. G. 1988*a* Contour surgery: a topological reconnection scheme for extended integrations using contour dynamics. *J. Comput. Phys.* **77**, 240–266.

DRITSCHEL, D. G. 1988*b* The repeated filamentation of two-dimensional vorticity interfaces. *J. Fluid Mech.* **194**, 511–547.

DRITSCHEL, D. G. 1995 A general theory for two-dimensional vortex interactions. *J. Fluid Mech.* **293**, 269–303.

DURAN-MATUTE, M., ALBAGNAC, J., KAMP, L. P. J. & VAN HEIJST, G. J. F. 2010 Dynamics and structure of decaying shallow dipolar vortices. *Phys. Fluids* **22**, 116606.

GAO, L. & YU, S. C. M. 2010 A model for the pinch-off process of the leading vortex ring in a starting jet. *J. Fluid Mech.* **656**, 205–222.

VAN GEFFEN, J. H. G. M. & VAN HEIJST, G. J. F. 1998 Viscous evolution of 2D dipolar vortices. *Fluid. Dyn. Res.* **22**, 191–213.

GHARIB, M., RAMBOD, E. & SHARIFF, K. 1998 A universal time scale for vortex ring formation. *J. Fluid Mech.* **360**, 121–140.

VAN HEIJST, G. J. F. & FLÓR, J. B. 1989 Dipole formation and collisions in a stratified fluid. *Nature* **340**, 212–215.

KAPLANSKY, F. B. & RUDI, Y. A. 2005 A model for the formation of 'optimal' vortex rings taking into account viscosity. *Phys. Fluids* **17**, 087101.

KELVIN, LORD 1880*a* On the vibrations of a columnar vortex. *Phil. Mag.* **10**, 155–168.

KELVIN, LORD 1880*b* Vortex statics. *Phil. Mag.* **10**, 97–109.

KERN, S. & KOUMOUTSAKOS, P. 2006 Simulations of optimized anguilliform swimming. *J. Expl Biol.* **209**, 4841–4857.

KHVOLES, R., BERSON, D. & KIZNER, Z. 2005 The structure and evolution of elliptical barotropic modons. *J. Fluid Mech.* **530**, 1–30.

KIM, D. & GHARIB, M. 2011 Flexibility effects on vortex formation of translating plates. *J. Fluid Mech.* **677**, 255–271.

KIZNER, Z. & KHVOLES, R. 2004 Two variations on the theme of Lamb-Chaplygin: supersmooth dipole and rotating multipoles. *Regular Chaotic Dyn.* **4**, 509–518.

KRUEGER, P. S., DABIRI, J. . O. & GHARIB, M. 2006 The formation number of vortex rings in uniform background coflow. *J. Fluid Mech.* **556**, 147–166.

KRUEGER, P. S. & GHARIB, M. 2003 The significance of vortex ring formation to the impulse and thrust of a starting jet. *Phys. Fluids* **15**, 1271–1281.

LINDEN, P. F. & TURNER, J. S. 2001 The formation of 'optimal' vortex rings, and the efficiency of propulsive devices. *J. Fluid Mech.* **427**, 61–72.

MAKAROV, V. G. & KIZNER, Z. 2011 Stability and evolution of uniform-vorticity dipoles. *J. Fluid Mech.* **672**, 307–325.

MOFFATT, H. K. & MOORE, D. W. 1978 The response of Hill's spherical vortex to a small axisymmetric disturbance. *J. Fluid Mech.* **168**, 337–367.

MOHSENI, K. & GHARIB, M. 1998 A model for universal time scale of vortex ring formation. *Phys. Fluids* **10**, 2436–2438.

NGUYEN DUC, J.-M. & SOMMERIA, J. 1998 Experimental characterization of two-dimensional vortex couples. *J. Fluid Mech.* **192**, 1175–1192.

NITSCHE, M. 2001 Self-similar shedding of vortex rings. *J. Fluid Mech.* **435**, 397–407.

NORBURY, J. 1973 A family of steady vortex rings. *J. Fluid Mech.* **57**, 417–431.

PAWLAK, G., CRUZ, C. M., BAZAN, C. M. & HRDY, P. G. 2007 Experimental characterization of starting jet dynamics. *Fluid Dyn. Res.* **39**, 711–730.

PEDRIZZETTI, G. 2010 Vortex formation out of two-dimensional orifices. *J. Fluid Mech.* **655**, 198–216.

PIERREHUMBERT, R. T. 1980 A family of steady, translating vortex pairs with distributed vorticity. *J. Fluid Mech.* **99**, 129–144.

POZRIKIDIS, C. 1986 The nonlinear instability of Hill's vortex. *J. Fluid Mech.* **168**, 337–367.

PULLIN, D. I. 1991 Contour dynamics methods. *Annu. Rev. Fluid Mech.* **24**, 84–115.

REUL, H., TALUKDER, N. & MULLER, W. 1981 Fluid mechanics of the natural mitral valve. *J. Biomech.* **14**, 361–372.

SAFFMAN, P. G. 1992 *Vortex Dynamics*. Cambridge University Press.

SAFFMAN, P. G. & SZETO, R. 1980 Equilibrium shapes of a pair of equal uniform vortices. *Phys. Fluids* **23**, 2339–2342.

SAFFMAN, P. G. & TANVEER, S. 1982 The touching pair of equal and opposite uniform vortices. *Phys. Fluids* **25**, 1929–1930.

SHARIFF, K., LEONARD, A. & FERZIGER, J. H. 2008 A contour dynamics algorithm for axisymmetric flow. *J. Comput. Phys.* **227**, 9044–9062.

SHUSSER, M. & GHARIB, M. 2000 Energy and velocity of a forming vortex ring. *Phys. Fluids* **12**, 618–621.

TRIELING, R., SANTBERG, R., VAN HEIJST, G. J. F. & KIZNER, Z. 2010 Barotropic elliptical dipoles in a rotating fluid. *Theor. Comput. Fluid Dyn.* **24**, 111–115.

VELASCO FUENTES, O. U. & VAN HEIJST, G. J. F. 1994 Experimental study of dipolar vortices on a topographic β-plane. *J. Fluid Mech.* **259**, 79–106.

WAN, Y.-H. 1988 Variational principles for Hill's spherical vortex and nearly spherical vortices. *Trans. Am. Math. Soc.* **308**, 299–312.

WIETING, D. W. & STRIPLING, T. E. 1984 Dynamics and fluid dynamics of the mitral valve. In *Recent Progress in Mitral Valve Disease* (ed. C. Duran, W. W. Angell, A. D. Johnson & J. H. Oury), pp. 13–46. Butterworths.

YE, Q. Y. & CHU, C. K. 1995 Unsteady evolutions of vortex rings. *Phys. Fluids* **7**, 795–801.

ZABUSKY, N. J., HUGHES, M. H. & ROBERTS, K. V. 1979 Contour dynamics for the Euler equations in two dimensions. *J. Comput. Phys.* **30**, 96–106.